

This is an Open Access document downloaded from ORCA, Cardiff University's institutional repository:<https://orca.cardiff.ac.uk/id/eprint/149846/>

This is the author's version of a work that was submitted to / accepted for publication.

Citation for final published version:

Zhang, Mengyuan, Shao, Longyi, Jones, Tim , Feng, Xiaolei, Ge, Shuoyi, Yang, Cheng-Xue, Cao, Yaxin, Berube, Kelly and Zhang, Daizhou 2022. Atmospheric iron particles in PM2.5 from a subway station, Beijing, China. *Atmospheric Environment* 283 , 119175. 10.1016/j.atmosenv.2022.119175

Publishers page: <https://doi.org/10.1016/j.atmosenv.2022.119175>

Please note:

Changes made as a result of publishing processes such as copy-editing, formatting and page numbers may not be reflected in this version. For the definitive version of this publication, please refer to the published source. You are advised to consult the publisher's version if you wish to cite this paper.

This version is being made available in accordance with publisher policies. See <http://orca.cf.ac.uk/policies.html> for usage policies. Copyright and moral rights for publications made available in ORCA are retained by the copyright holders.



1 **Atmospheric iron particles in PM_{2.5} from a subway station,**
2 **Beijing, China**

3 Mengyuan Zhang ^a, Longyi Shao ^{a*}, Tim Jones ^b, Xiaolei Feng ^a, Shuoyi Ge ^a,
4 Cheng-Xue Yang ^c, Yaxin Cao ^a, Kelly Bérubé ^d, Daizhou Zhang ^e

5 ^a State Key Laboratory of Coal Resources and Safe Mining, College of Geoscience and
6 Survey Engineering, China University of Mining and Technology (Beijing), Beijing
7 100083, China

8 ^b School of Earth and Environmental Sciences, Cardiff University, Park Place, Cardiff,
9 CF10, 3YE, UK

10 ^c Institute of Earth Sciences, China University of Geosciences Beijing, Beijing 100083,
11 China

12 ^d School of Biosciences, Cardiff University, Museum Avenue, Cardiff, CF10 3AX,
13 Wales, UK

14 ^e Faculty of Environmental and Symbiotic Sciences, Prefectural University of
15 Kumamoto, Kumamoto, 62-8502, Japan

16 *Correspondence: ShaoL@cumtb.edu.cn

17
18 **Highlights:**

- 19 • The majority of PM_{2.5} in the subway's atmosphere are Fe-rich particles.
20 • Fe-rich particles are mainly derived from mechanical abrasion at the brake-wheel-
21 rail interfaces.
22 • The Fe-rich particles typically exist as Fe-Mn alloy fragments.

23

24 **Abstract:**

25 Particulate matter pollution in the subway station's atmosphere can seriously influence
26 the air quality and impacts on the health of subway workers and commuters. In this
27 study, PM_{2.5} samples were collected from different locations within a subway station in
28 Beijing, and the individual particles were analyzed for morphology and composition by
29 Transmission Electron Microscopy with Energy Dispersive X-ray Spectrometry (TEM-
30 EDX). The results showed that the concentration of PM_{2.5} in subway stations was
31 affected by both indoor and outdoor sources. Particles generated by train-related
32 sources such as resuspension, wheel, rail, brake and collector shoe abrasion were a
33 significant source of airborne pollution in the subway atmosphere. Within the subway
34 station PM_{2.5}, Fe was the dominant element, and was detected in more than 75% of all
35 particles analyzed. The Fe-rich particles were identified in railway carriages (79.4%),
36 station concourse (65.3%), and platforms (61.3%). The geometric mean diameter of Fe-
37 rich particles was 0.34 μm, which was smaller than that of all detected particles. Cr, Mn
38 and other metals were often detected in the Fe-rich particles, reflecting metal alloys
39 used in the wheels and tracks. A better understanding of the particle distribution around
40 different areas of the subway system and the physicochemical characteristics of these
41 Fe-rich particles is critical in developing a meaningful assessment of the risk posed by
42 particles in the subway atmosphere.

43

44 **Keywords:** Subway atmospheric pollution, PM_{2.5}, TEM-EDX, Individual particle
45 analyses, Fe-alloy metals

46

47 **1. Introduction**

48 Globally, subways are crucial public transportation systems in megacities, because
49 of their convenience, safety, efficiency, and large passenger capacity (Chang, et al.,
50 2021). However, the subway environments are usually composed of confined and
51 artificially ventilated spaces, resulting in restricted air flow and concentration of
52 airborne pollutants within the station. The concentration of these pollutants will be a

53 function of many factors such as operation times, depth, design style or the efficiency
54 of ventilation system. A number of studies that have been conducted in subway stations
55 showed that PM_{2.5} might accumulate to 2-10 times higher levels than in the ambient air
56 outside the stations (Reche et al., 2017; Chang et al., 2021). Cao et al. (2017) reported
57 that the average PM_{2.5} mass concentration at an underground platform of the Suzhou
58 subway station in the southeastern Jiangsu Province of eastern China was 142 µg/m³,
59 which was higher than the second-level concentration limit for the ambient air (75µg/m³)
60 stipulated by the National Ambient Air Quality Standards (GB3095–2012). Martins et
61 al. (2016) noted that in the Barcelona, Spain, subway system the average PM_{2.5}
62 concentrations in the subway platforms atmosphere were between 1.4 and 5.4 times
63 higher than that found outdoors.

64 Many studies have shown that the chemical composition of PM_{2.5} in subways
65 consisted mainly of the metal elements including Fe, Mn, Mg, Pb, Na, Cr, K, Cu, Ca,
66 Zn, Ba, Ni, V and the non-metallic elements such as C, O, S, and Si (Kamani et al.,
67 2014; Moreno et al., 2014; Byeon et al., 2015). Among the metallic elements, Fe was
68 the most common in the PM_{2.5} of subways (Midander et al., 2012; Mohsen et al., 2018).
69 When compared with local outdoor PM_{2.5} pollution, the Fe content in the subway tunnel
70 was almost twice that measured in the outdoor air (Pan et al., 2019). These iron particles
71 from subway stations were discharged into the ambient atmosphere through the
72 ventilation systems and might have an impact on human health and geochemical cycles
73 (Li et al., 2017; Zhu et al., 2020).

74 Metal particles can pose potential respiratory health risks to commuters and
75 workers in subway stations (Canu et al., 2021; Hwang et al., 2021). A study in Canada
76 evaluated the exposure risk to the commuter in the subway, which indicated that the
77 commuters were exposed to PM_{2.5} containing several heavy metals in the subway
78 system every day, especially to Fe that accounts for 80%-99% (Van Ryswyk et al., 2017).
79 The metal components of PM_{2.5} can be solubilized once respired, and generate Reactive
80 Oxygen Species (ROS), which can induce oxidative stress and inflammation in the
81 lungs and respiratory tract (Kumar et al., 2018; Palleschi et al., 2018). There is also a
82 synergy between certain metals resulting in a toxic cocktail, which is more harmful than

83 the toxic sum of the individual metals (Merolla and Richards, 2005). Gali et al. (2017)
84 and Moreno et al. (2017) reported the oxidative potential of PM_{2.5} samples collected
85 from the subway system in Hong Kong and Barcelona. Their results indicated that
86 subway PM toxicity might be affected by the presence of metal elements sourced from
87 the alloys used in the mechanical components of the system.

88 Although several studies have reported the concentration, distribution and toxicity
89 of metallic particles in the subway stations, these results cannot directly reveal the
90 source of pollution and mechanism of toxicology (Kelly et al., 2012; Xiao et al., 2020;
91 Ji et al., 2021; Saeedi et al., 2021). The morphology, elemental composition and size
92 are the key factors determining the source and toxicity of particles (Li et al., 2020; Wang
93 et al., 2022). However, no detailed targeted work has been done to characterize the
94 physicochemical characteristics of Fe-rich particles. Individual particle analysis
95 technology based on TEM-EDX which make up for the disadvantages of previous
96 research, can obtain the morphology, element composition, and size of individual
97 particle to analyze the surface elements occurrence state, and source of particles (Shao
98 et al., 2022b).

99 In this study, individual particles were collected from different locations within the
100 LiuDaoKou (LDK) subway station in northwestern urban Beijing, under different
101 pollution conditions. The occurrence, form and spatial distribution of Fe-rich particles
102 in PM_{2.5} were studied by TEM-EDX, and the results provide important insights into the
103 nature of the subway air pollution, and additionally data for risk assessments on the
104 respiratory health of subway workers and commuters.

105

106 **2. Material and methods**

107 **2.1 Study area**

108 The LDK subway station of line 15 opened in 2014. The full height screen door is
109 fitted between the platform and the tunnel. In this subway station, the air flow is
110 separated by the screen door, except when the doors are open or the seals are broken.
111 All the stations have air conditioning, which is connected to the surface ventilation shaft

112 to exchange fresh air from outside with the station air. The LDK subway station is one
 113 of the newest types of stations in Beijing which has more advanced ventilation and
 114 screen doors than the older stations of line 1. Therefore, this study chose the LDK
 115 station as the sampling site.

116 The LDK station has two-level underground floors. The sampling sites at (A)
 117 carriage, (B) platforms, (C) concourse, and (D) exit are showed in Fig. 1.

118 A. Carriage: The sampling point is located in the middle of a train carriage,
 119 approximately 20 metres from the joints to the connecting carriages, and 2
 120 metres from the door.

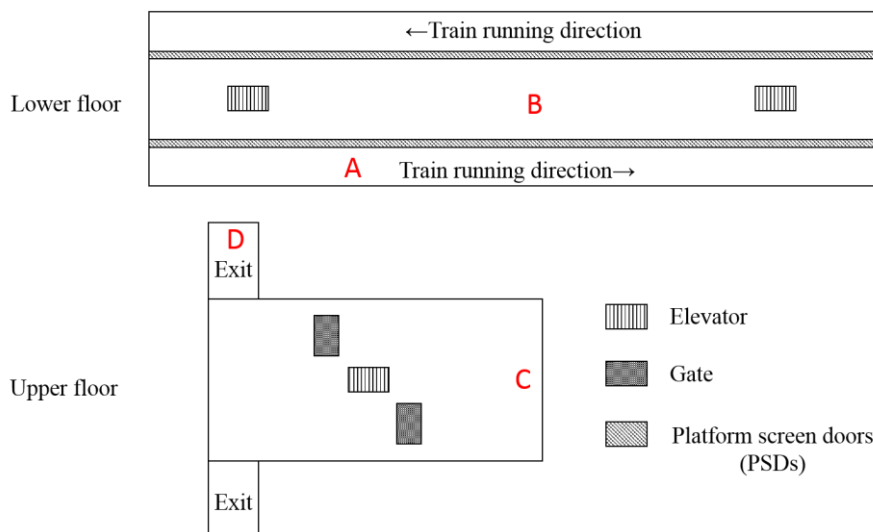
121 B. Platform: The sampling point is located in the center of the platform at the
 122 lower floor, approximately 3-4 metres from the platform screen doors and 100
 123 metres from the escalators on both sides.

124 C. Concourse: The sampling point is located at the side of the concourse at the
 125 upper floor, approximately 50 metres from the main entrance and escalator.

126 D. Exit: The exit is located on the surface, connecting the station to the outside
 127 environment. The sampling point is located at the upper end of the exit
 128 escalator, approximately 10 metres from the escalator.

129 The sampling was undertaken during off-peak hours, and the average frequency of
 130 trains was every 3-4 minutes.

131



132

133 Fig.1. Plain view of two floors for the localities of the sampling sites (A: Carriage, B:

Platform, C: Concourse, D: Exit)

2.2 Aerosol sampling

A single-stage cascade PM sampler (DKL-2, Qingdao Jinshida Company, China) was used at a flow rate of 1.0 L/min to collect the particle samples under different pollution conditions in September 2018. According to the second-level concentration limit for the ambient air stipulated by the National Ambient Air Quality Standards (GB3095–2012), we defined the days with $PM_{2.5}$ concentrations higher than $75\mu\text{g}/\text{m}^3$ as haze days and lower than $75\mu\text{g}/\text{m}^3$ as non-haze days.

Copper TEM grids with carbon-coated organic film (300-mesh copper, T10023, Beijing Xinxingbairui Company, China), placed inside the PM sampler, were used. The Kestrel 5500 Pocket Weather Tracker (Nielsen-Kellerman Inc., Minneapolis, MN, USA) was synchronously used to measure the relative humidity (RH) and temperature (T).

A $PM_{2.5}$ detector (SDL301, China) was used to monitor the average real-time concentrations of $PM_{2.5}$ at the sites of the exit, concourse, platform and carriage inside the subway station. The time interval of collection was 1s, and more than 500 data points were collected from the same sampling sites.

The hourly average concentrations of $PM_{2.5}$, SO_2 , NO_2 and O_3 in the ambient atmosphere outside the subway station were obtained from the Wanliu monitoring station (<http://www.bjmemc.com.cn/>) in Haidian district (116.287E, 39.987N; 5km from the subway station).

2.3 Individual-particle analysis

TEM-EDX (JEM2800, JEOL, Japan, 200 kV) was used to analyze the morphology and elemental composition of individual particles. Only elements with an atomic number larger than 5(B) were detected by the EDX. In order to ensure the collection of all possible elements and minimize the omission of volatile elements, the collection time of EDX spectra was 20-90s. Since the TEM grids are made of copper, Cu was excluded from the analysis.

To ensure that the analyzed particles were representative of the whole sample, at

164 least 90 particles from 2-3 random areas were analyzed on each grid. Considering the
165 collection efficiency of the impactor, particles smaller than 0.1 μm are not counted. An
166 image processing system (Microscopic Particle Size of Digital Image Analysis System,
167 UK) was used to measure the surface areas of particles. According to the circle area
168 formula, the equivalent spherical diameter of a particle was calculated by $\sqrt{S/4\pi}$,
169 where S was the surface area. To compare the size of different types of particles, the
170 following formula was used to calculate the geometric mean diameter (D_{gm}) of particles:

$$171 \quad D_{\text{gm}} = (D_1 \cdot D_2 \cdot D_3 \cdots D_n)^{\frac{1}{n}}$$

172 where n represents numbers of particles.

173

174 **3. Results**

175 **3.1 Mass concentration of air pollutants**

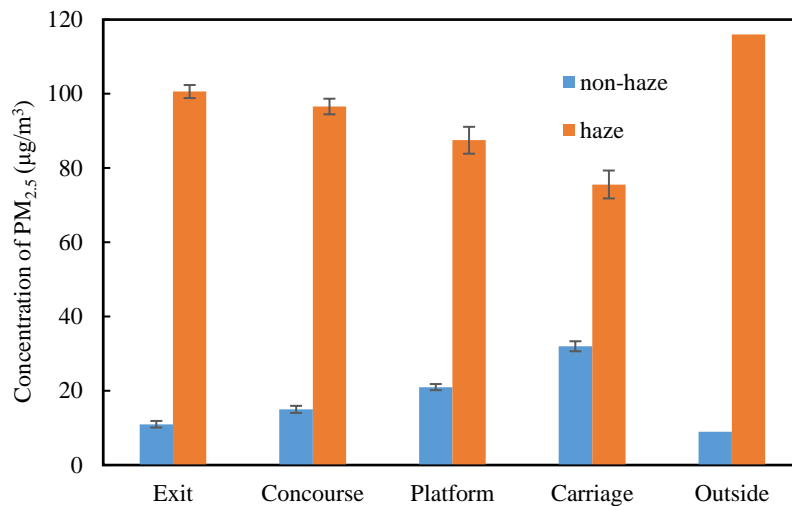
176 The results of the average real-time concentration of $\text{PM}_{2.5}$ at the different locations
177 in the subway station and outside environment during haze and non-haze days are
178 presented in Fig. 2.

179 On haze days, the average concentration of $\text{PM}_{2.5}$ in the atmosphere inside the
180 subway station was $90 \pm 3 \mu\text{g}/\text{m}^3$ and was 22% lower than the outside environment $\text{PM}_{2.5}$
181 concentrations. The concentration of $\text{PM}_{2.5}$ at the exit site was the highest, being
182 $101 \pm 1.8 \mu\text{g}/\text{m}^3$, and that at the carriage site was the lowest, being $76 \pm 3.8 \mu\text{g}/\text{m}^3$. The
183 concentration of $\text{PM}_{2.5}$ at different locations in the station from high to low was exit >
184 concourse > platform > carriage.

185 On non-haze day, the inside subway station atmosphere showed an average $\text{PM}_{2.5}$
186 concentration of $20 \pm 1 \mu\text{g}/\text{m}^3$ and was 1.2 times higher than the outside atmosphere
187 $\text{PM}_{2.5}$ concentration. The concentration of $\text{PM}_{2.5}$ in the carriage was the highest, at
188 $32 \pm 1.3 \mu\text{g}/\text{m}^3$ and in the exit the lowest at $11 \pm 0.9 \mu\text{g}/\text{m}^3$. The concentration of $\text{PM}_{2.5}$ at
189 different locations in the station from high to low was carriage > platform > concourse >
190 exit.

191 Overall, the results showed that the concentrations of $\text{PM}_{2.5}$ in the subway station
192 were lower than that in the outside air during haze days. However, during non-haze

193 days, the concentrations of PM_{2.5} in the subway station were higher than those in outside
194 air. This result was consistent with those reported by Pan et al. (2019) who concluded
195 that the pollution in subway stations varies over a wide range compared with the outside
196 environment.



197

198 Fig. 2. The concentration of PM_{2.5} at different locations in the subway station and
199 outside environment during haze and non-haze days

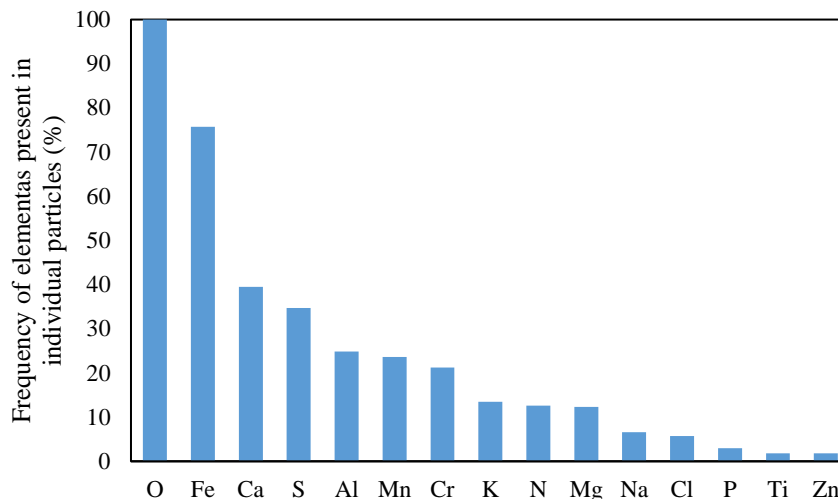
200

201 3.2 Frequency of elements in individual particles

202 The particles collected in the subway station show complex compositions. TEM-
203 EDX has detected more than 16 elements in the particles, including N, O, Na, Mg, Al,
204 P, S, Cl, K, Ca, Ti, Cr, Mn, Fe, and Zn (Fig. 3).

205 In the subway station particles, except for O, Fe was the most abundant element,
206 and was detected in more than 75% of all the analyzed particles. The abundance of Ca
207 and S was next to Fe, and these elements were detected in more than 30% of all the
208 analyzed particles. More than 75% of the particles contained metallic elements,
209 including Fe, Mn, and Cr. Our results closely compared with those reported by Van
210 Ryswyk et al. (2017) where Fe and Mn were the most abundant metals in the Toronto
211 and Vancouver subway atmospheric pollution. Metallic elements have generally been
212 identified as potentially hazardous components in the airborne particles
213 (MohseniBandpi et al., 2018; Guo et al., 2021), and these particles present in subway
214 station air could present health risks to the people commuting in the subway station.

215 Once these particles are discharged into the proximal surface atmosphere by the
 216 ventilation systems, they could further increase the health risk to people outside the
 217 subway.



218
 219 Fig. 3. Frequency of elements present in the collected aerosol particles in the subway
 220 station.

221
 222

223 3.3 Classification and number fractions of individual particles

224 A total of 344 particles were analyzed from the subway station. Based on their
 225 morphology and elemental composition, the particles in subway station air were
 226 classified into types of metal, mineral, S-rich, organic and salt particles. Detailed
 227 characteristics of different types of individual particles are shown in Table 1.

228 Table 1: Types and characteristics of individual particles in subway station air

Particle types	Major elements	Possible source
Metal	Composed of Fe and O, and minor Cr and Zn	Rail, wheel, and brake wear (Minguillon et al., 2018; Salma et al., 2007)
Mineral	Composed of Si and O, and minor Ca, Mg, Al	Wear and resuspension of building materials in the subway system (Jung et al., 2010)
S-rich	Composed of S, N, O	Secondary formation in atmosphere (Shao et al., 2022b)

Organic	Composed of C and O, and minor S	Trains, escalators and passengers (Van Drooge et al., 2018; Shao et al., 2022a)
Mixture	Complex elemental composition	Secondary chemical reaction (Shao et al., 2022b)

229

230 Metal particles have irregular shapes, among which the Fe-rich particles (Fig. 4a,
231 b, d, e) are the most common. The metal particles in the subway station are identified
232 to be emitted from brake wear, rail-wheel' friction (Minguillon et al., 2018) and rubbing
233 of bow sliding collectors and the electric conducting rail (Salma et al., 2007).

234 Mineral particles are irregular in shape (Fig. 4g) with the major elements such as
235 Si, Al, and Ca (Fig. 4h), which are identified as crustal elements. Mineral particles are
236 extremely stable and non-volatile under the strong electron beam. Mineral particles
237 include a large number of silicate minerals, which are thought to have originated from
238 wear and resuspension of building materials in the subway system and raised by the
239 piston wind (Jung et al., 2010).

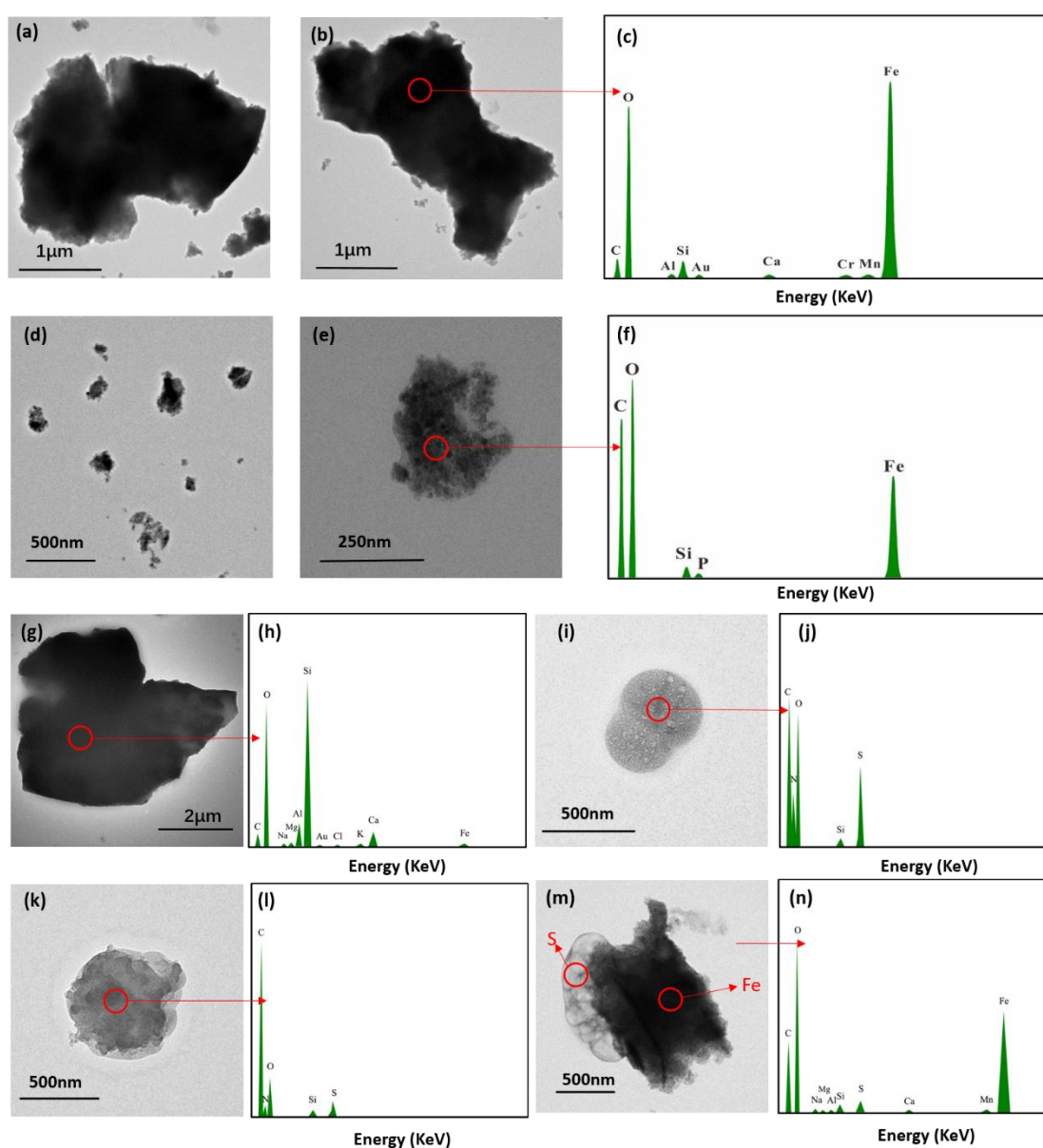
240 The S-rich particles mainly consist of ammonia sulfate and have irregular or
241 spherical shapes (Fig. 4i), and these type of particles tend to be formed by the secondary
242 chemical reactions in the atmosphere (Shao et al., 2022b). These sulfate particles, which
243 easily volatilize under the electron beam have a 'foam-like' morphology after
244 volatilizing.

245 Organic particles have spherical or nearly spherical shapes (Fig. 4k). Unlike S-rich
246 particles, organic particles are extremely stable and non-volatile under the strong
247 electron beam. Van Drooge et al. (2018) have reported that the majority of organic
248 particles in the platforms originate from outdoor air. In the outside atmospheric
249 environment, organic particles are mainly emitted from fossil fuels and biomass
250 burning (Shao et al., 2022b). In addition to those transported from external environment,
251 there are also a number of sources of organic particles from trains, escalators and
252 passengers in subway system (Van Drooge et al., 2018; Shao et al., 2022a).

253 Particles in the atmosphere often don't exist as a single phase of chemical

254 composition. For example, due to the high humidity in haze weather, the chemical
255 reaction between particles is more intense than that in non-haze days (Shao et al.,
256 2022b). Under these conditions, particles tend to appear in a mixed state by the
257 secondary chemical reactions in the atmosphere (Xing et al., 2020). Mixed particles are
258 irregular in shape and show inhomogeneous internal structures (Fig. 4m). Sulfate
259 particles mixed with metal particles were the most common among all detected mixture
260 particles in this study.

261



262

263 Fig. 4. Examples of morphologies under TEM, and mixing characteristics of
264 individual particles in subway station. (a-b, d-e) Fe-rich particle, panels (c) and (f) are

265 EDX of (b) and (e); (g) Si-rich mineral particle, panel (h) is EDX of (g); (i) S-rich
266 particle, panel (j) is EDX of (i); (k) organic particle, panel (l) is EDX of (k); (m) S-Fe
267 mixture particle, panel (n) is EDX of (m)
268

269 The relative percentage of the different types of individual particle inside and
270 outside the subway station is shown in Fig. 5.

271 The composition of PM_{2.5} differed under the different pollution conditions. Metal
272 particles were predominant in the subway station atmosphere during haze and non-haze
273 days, accounting for 39.0% and 53.4% respectively. Inside the station, the relative
274 percentages of metal particles were much higher than the outside atmosphere, and it has
275 been reported by Shao et al. (2021) that the relative percentages of metal particles in
276 outside ambient air during haze and non-haze day were 2.7% and 0.3% respectively.
277 The S-rich particles were only found in the samples during the haze days, accounting
278 for 30%. A number of studies have reported the high percentage of S-rich particles in
279 the environmental atmosphere during haze days (Wang et al. 2022; Shao et al. 2021).
280 Therefore, the S-rich particles detected in this study were mainly sourced from the
281 outside environment.

282 The relative percentages of the different types of particles varied in different areas
283 of the subway station. Metal particles were abundant at the carriages (79.4%),
284 concourse (65.3%) and platform (61.3%). At the exit site, the mineral particles were the
285 major particle type, accounting for 92.3%, which could be attributed to crustal dust
286 resuspension.

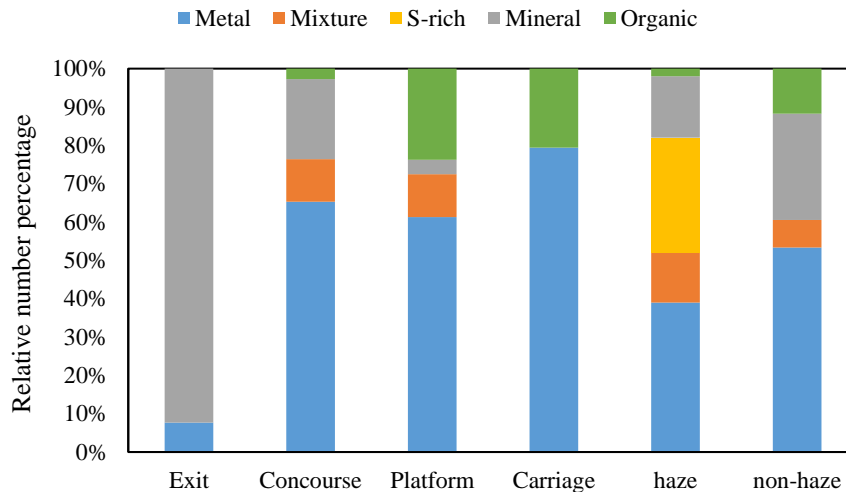


Fig. 5. Relative number percentages of individual particles in the subway station.

4. Discussion

4.1 Factors affecting PM_{2.5} in the subway station

The PM_{2.5} in the subway station is influenced by both indoor and ambient outdoor sources. Indoor sources include the resuspension of dust particles due to the passengers or train movements, and the mechanical abrasion emissions, such as between the train wheels and rails (Li et al., 2018). Ambient outdoor sources refer to the local air quality and pollution from vehicles, industry and combustion sources.

The pollution in the subway station varies over a wide range, as also seen with the outside atmospheric pollution (Zhao et al., 2017; Lee et al., 2018). In general, the concentrations of PM_{2.5} were higher during the haze days than during non-haze days. During haze days the concentrations of PM_{2.5} inside the subway station were lower than the those outside, which indicated that outside ambient sources were the main pollution contributors. On the contrary, during the non-haze days the indoor sources were the main components. Moreover, ranking the PM_{2.5} concentrations of the different areas of the subway system during the non-haze days showed that carriage > platform > concourse > exit, which also indicated that the smaller distance to the rail track will be associated with the higher PM_{2.5} concentrations in the subway station. This indicated that particles from train-related sources such as resuspension, wheel, rail, brake and collector shoe abrasion were the major factor causing environmental pollution inside

309 the subway.

310

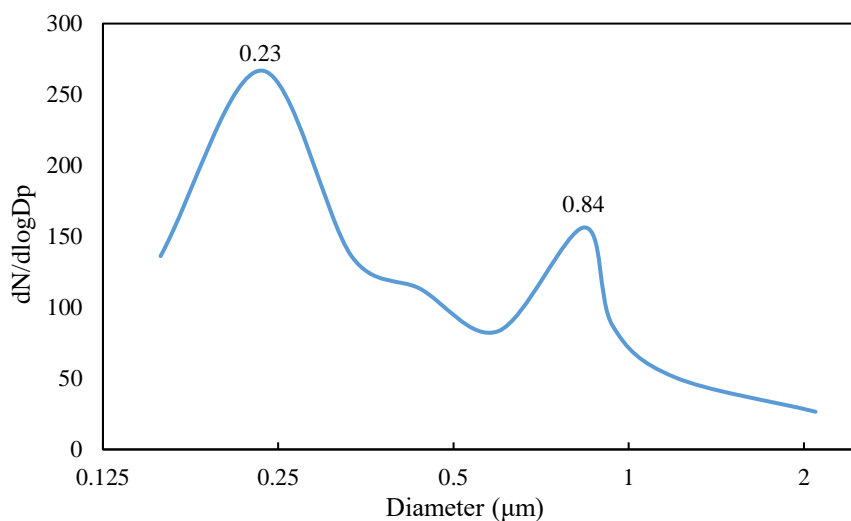
311 **4.2 Morphology and chemistry of Fe-rich particles in subway air**

312 From the high-resolution TEM images, it is shown that the Fe-rich particles mainly
313 exist in two morphologies. The first is the homogeneous Fe-rich fragments (Fig. 4a and
314 4b), typically with torn and ragged edges. The second is the heterogeneous Fe-rich
315 fragments, which interpreted as a large number of tiny Fe-rich fragments aggregate (Fig.
316 4d and 4e).

317 The two different morphologies may represent either an aging (oxidation) process
318 or is a result of the mode of formation. A study by Moreno et al. (2015) suggested that
319 Fe-rich flakes and splinters are released by mechanical wear at the brake-wheel and
320 wheel-rail interfaces. The oxidation of these particles results in extensive alteration of
321 the structure to more rounded aggregates, with iron metal flakes still preserved in some
322 particle cores (Moreno et al., 2015). The presence of Mn is good evidence that the
323 particles are largely generated from the train rails as Fe-Mn alloy, or 1084 rolled steel,
324 is commonly used in railway tracks, and the addition of 0.7-1.0% Mn significantly
325 improves the anti-wear properties (Dhar et al., 2020).

326 The analytical technique used in this study does not allow a determination of
327 whether the Fe-rich particles are pure metal or metal oxide. The TEM-EDX spectra
328 showed significant peaks for oxygen. This oxygen could be from the organic film used
329 to support the particles for TEM, or also could come from metal oxides, predominantly
330 Fe oxide. We can speculate that the Fe-rich particles may result from metal-on-metal
331 abrasion. When the train brakes are applied, the resulting abrasion will generate minute
332 Fe particles as well as heat (Martins et al., 2016; Moreno et al., 2017). Once generated,
333 these particles will start to oxidize or rust, and they will either be directly suspended
334 into the atmosphere by the strong air movements created by moving trains, or be
335 deposited in the places proximal to the tracks where the potential of re-suspension into
336 the atmosphere exists with every passing train (Jung et al., 2010). On some occasions,
337 more aggressive braking can generate sparks, which are presumably the Fe-rich
338 particles being instantly oxidized (Namgung et al., 2017). It is therefore likely that the

339 Fe-rich particles in the subway atmosphere will usually be “Fe oxide”-rich particles. Fe
340 oxides are generally stable in the air as Fe₂O₃, which is the main component of hematite.
341 It agrees with the conclusions reported by Moreno et al. (2015) that Fe-rich particles
342 undergo progressive atmospheric oxidation from metal Fe to hematite.



343

344 Fig. 6. Number-size distribution of Fe-rich particles in subway station air from the
345 TEM analysis.

346

347 Fig. 6 illustrates the number ($dN/d\log D_p$) - size distributions of Fe-rich particles in
348 the subway station air, where N is the relative number fraction and D_p is the equivalent
349 diameter. The Fe-rich particles were in the size range of 0.1-2.78 μm and displayed a
350 bimodal distribution, with one peak at 0.23 μm and another at 0.84 μm . According to
351 TEM analysis, the Fe-rich particles mainly exist in two morphologies, with the
352 homogeneous Fe-rich fragments (Fig. 4a and 4b) and the heterogeneous Fe-rich
353 fragments (Fig. 4d and 4e). The mean diameter of the homogeneous Fe-rich fragments
354 was around 0.84 μm , while the heterogeneous Fe-rich fragments was around 0.23 μm .
355 Therefore, the bimodal distribution of Fe-rich particles is consistent with the
356 morphology characteristics.

357

358 In general, Fe-rich particles collected at different sites of the subway showed the
359 consistent number-size distribution (Fig. S1). The geometric mean diameter of all Fe-
360 rich particles was around 0.34 μm , which was smaller than all detected particles at 0.47
 μm . Submicron particles (equivalent diameter less than 1 μm) accounted for 89.5% of

361 all Fe-rich particles, indicating that most of the Fe-PM_{2.5} in the subway air exists in
362 smaller size ranges.

363 Several studies have shown that the form of metals in airborne particles can have
364 important implications for human health (Zelikoff et al., 2002; Gilli et al., 2007; von
365 Schneidmesser et al., 2010). Particles with smaller sizes are of more concern due to
366 being more respirable, their relatively larger surface area and strong adsorption capacity
367 (Al-Dabbous and Kumar, 2014; Olawoyin et al., 2018). Therefore, smaller respirable
368 particles could present a higher health risk than larger particles (Feng et al., 2020; Pan
369 et al., 2019). In addition, for the metal particles the detection frequency of Fe-Mn alloy
370 particles is the highest (47.6%), which is consistent with the composition of manganese
371 steel used in modern subway tracks (Dhar et al., 2020). Merolla and Richards (2005)
372 have reported that when particulate matter contains multiple metals, the combined
373 holistic toxic effects can exacerbate the health risk to human beings. Therefore, the
374 large number of Fe-Mn alloy fragments with small particle size and potential toxicity
375 in the subway system should attract our attention.

376

377 **5. Conclusions**

378 The concentration of PM_{2.5} in subway stations was affected by both indoor
379 generated and outdoor ambient sources. In this study, we noted that during the non-haze
380 days, the concentrations of PM_{2.5} inside subway station were higher than that found
381 outside. However, during the haze days, the relationship was reversed. The train-related
382 sources such as resuspension, wheel, rail, brake and collector shoe abrasion were the
383 main cause of Fe-rich particulate pollution in the subway air.

384 Within the subway station, the Fe-rich particles were most abundant, and Fe was
385 detected in more than 75% of all analyzed particles. The Fe-rich particles were abundant
386 in the sites of carriages (79.4%), concourse (65.3%) and platform (61.3%).

387 The Fe-rich particles were in the size range of 0.1-2.78 μm , and the geometric mean
388 diameter of the Fe-rich particles was around 0.34 μm , which was smaller than that for
389 all detected particles, 0.47 μm . Cr and Mn were often detected with the Fe, which has
390 implications for the potential respiratory toxicity of subway airborne particulate matter.

391 A better understanding of the particle distribution around different areas of the
392 subway system and the physicochemical characteristic of these Fe-rich particles is
393 critical in developing a meaningful assessment of the risk posed by particles in the
394 subway atmosphere.

395

396 **Acknowledgments**

397 This study is supported by the National Natural Science Foundation of China
398 (Grant No. 42075107) and the Fundamental Research Funds for the Central
399 Universities (Grant No. 2022YJSDC05).

400

401 **Reference:**

- 402 Al-Dabbous, A.N., Kumar, P., 2014. Number and size distribution of airborne
403 nanoparticles during summertime in kuwait: first observations from the middle east.
404 *Environ. Sci. Technol.* 48 (23), 13634-13643.
- 405 Byeon, S.H., Willis, R., Peters, T.M., 2015. Chemical characterization of outdoor and
406 subway fine PM_{2.5-1.0} and coarse PM_{10-2.5} particulate matter in seoul korea by
407 computer-controlled Scanning Electron Microscopy (CCSEM). *Int. J. Env. Res.*
408 *Pub. He.* 12 (2), 2090-2104.
- 409 Canu, I.G., Creze, C., Hemmendinger, M., Ben Rayana, T., Besancon, S., Jouannique,
410 V., Debatisse, A., Wild, P., Sauvain, J.J., Suarez, G., Hopf, N.B., 2021. Particle and
411 metal exposure in Parisian subway: Relationship between exposure biomarkers in
412 air, exhaled breath condensate, and urine. *Int. J. Env. Res. Pub. He.* 237, 113837.
- 413 Cao, S.J., Kong, X.R., Li, L., Zhang, W., Ye, Z.P., Deng, Y., 2017. An investigation of
414 the PM_{2.5} and NO₂ concentrations and their human health impacts in the metro
415 subway system of Suzhou, China. *Environ. Sci-Proc. Imp.* 19 (5), 666-675.
- 416 Chang, L., Chong, W.T., Wang, X.R., Pei, F., Zhang, X.X., Wang, T.Z., Wang, C.Q., Pan,
417 S., 2021. Recent progress in research on PM_{2.5} in subways. *Environ. Sci-Proc.*
418 *Imp.* 23 (5), 642-663.
- 419 Dhar, S., Ahlstrom, J., Zhang, X., Danielsen, H.K., Jensen, D.J., 2020. Multi-axial
420 fatigue of head-hardened pearlitic and austenitic manganese railway steels: a
421 comparative study. *Metall. Mater. Trans. A.* 51 (11), 5639-5652.
- 422 Feng, X.L., Shao, L.Y., Xi, C.X., Jones, T., Zhang, D.Z., BeruBe, K., 2020. Particle-
423 induced oxidative damage by indoor size-segregated particulate matter from coal-
424 burning homes in the Xuanwei lung cancer epidemic area, Yunnan Province, China.
425 *Chemosphere* 256, 127058.
- 426 Gali, N.K., Jiang, S.Y., Yang, F., Sun, L., Ning, Z., 2017. Redox characteristics of size-
427 segregated PM from different public transport microenvironments in Hong Kong.
428 *Air Qual. Atmos. Hlth.* 10 (7), 833-844.

- 429 Gilli, G., Traversi, D., Rovere, R., Pignata, C., Schiliro, T., 2007. Chemical
430 characteristics and mutagenic activity of PM₁₀ in Torino, a northern Italian City.
431 *Sci. Total Environ.* 385 (1-3), 97-107.
- 432 Guo, G.H., Zhang, D.G., Wang, Y.T., 2021. Characteristics of heavy metals in size-
433 fractionated atmospheric particulate matters and associated health risk assessment
434 based on the respiratory deposition. *Environ. Geochem. Hlth.* 43 (1), 285-299.
- 435 Hwang, S., Kim, S., Choi, S., Lee, S., Park, D., 2021. Correlation between levels of
436 airborne endotoxin and heavy metals in subway environments in South Korea. *Sci.*
437 *Rep-UK* 11 (1), 17086.
- 438 Ji, W.J., Liu, C.H., Liu, Z.Z., Wang, C.W., Li, X.F., 2021. Concentration, composition,
439 and exposure contributions of fine particulate matter on subway concourses in
440 China. *Environ. Pollut.* 275, 116627.
- 441 Jung, H.J., Kim B., Ryu, J., Maskey, S., Kim, J.C., Sohn, J., 2010. Source identification
442 of particulate matter collected at underground subway stations in Seoul, Korea
443 using quantitative single-particle analysis. *Atmos. Environ.* 44 (19), 2287-2293.
- 444 Kamani, H., Hoseini, M., Seyedsalehi, M., Mahdavi, Y., Jaafari, J., Safari, G., 2014.
445 Concentration and characterization of airborne particles in Tehran's subway system.
446 *Environ. Sci. Pollut. R.* 21 (12), 7319-7328.
- 447 Kelly, F., Fussell, J., 2012. Size, source and chemical composition as determinants of
448 toxicity attributable to ambient particulate matter. *Atmos. Environ.* 60, 504-526.
- 449 Kumar, S.S., Muthuselvam, P., Pugalenti, V., Subramanian, N., Ramkumar, K.M.,
450 Suresh, T., Suzuki, T., Rajaguru, P., 2018. Toxicoproteomic analysis of human lung
451 epithelial cells exposed to steel industry ambient particulate matter (PM) reveals
452 possible mechanism of PM related carcinogenesis. *Environ. Pollut.* 239, 483-492.
- 453 Lee, Y., Lee, Y. C., Kim, T., Choi J. S., Park, D., 2018. Sources and characteristics of
454 particulate matter in subway tunnels in Seoul, Korea. *Int. J. Env. Res. Pub. He.* 15
455 (11), 2534.
- 456 Li, W.J., Sun, J.X., Xu, L., Shi, Z.B., Riemer, N., Sun, Y.L., Fu, P.Q., Zhang, J.C., Lin,
457 Y.T., Wang, X.F., 2016. A conceptual framework for mixing structures in individual
458 aerosol particles. *J. Geophys. Res. Atmos.* 121 (22), 13784-13798.
- 459 Li, W.J., Xu, L., Liu, X.H., Zhang, J.C., Lin, Y.T., Yao, X.H., Gao, H.W., Zhang, D.Z.,
460 Chen, J.M., Wang, W.X., Harrison, R.M., Zhang, X.Y., Shao, L.Y., Fu, P.Q., Nenes,
461 A., Shi, Z.B., 2017. Air pollution-aerosol interactions produce more bioavailable
462 iron for ocean ecosystems. *Sci. Adv.* 3(3), 1601749.
- 463 Li, Y.W., Shao, L.Y., Wang, W.H., Zhang, M.Y., Feng, X.L., Li, W.J., Zhang, D.Z., 2020.
464 Airborne fiber particles: Types, size and concentration observed in Beijing. *Sci.*
465 *Total Environ.* 705, 135967.
- 466 Li, Z.Y., Che, W.W., Frey, H.C., Lau, A.K.H., 2018. Factors affecting variability in
467 PM_{2.5} exposure concentrations in a metro system. *Environ. Res.* 160, 20-26.
- 468 Liu, L., Kong, S.F., Zhang, Y.X., Wang, Y.Y., Xu, L., Yan, Q., Lingaswamy, A.P., Shi,
469 Z.B., Lv, S.L., Niu, H.Y., Shao, L.Y., Hu, M., Zhang, D.Z., Chen, J.M., Zhang, X.Y.,
470 Li, W.J., 2017. Morphology, composition, and mixing state of primary particles
471 from combustion sources – crop residue, wood, and solid waste. *Sci. Rep.* 7, 5047.
- 472 Martins, V., Moreno, T., Cruz Minguillon, M., van Drooge, B.L., Reche, C., Amato, F.,

473 de Miguel, E., Capdevila, M., Centelles, S., Querol, X., 2016. Origin of inorganic
474 and organic components of PM_{2.5} in subway stations of Barcelona. Spain. *Environ.*
475 *Pollut.* 208, 125-136.

476 Merolla, L., Richards, R.J., 2005. In vitro effects of water-soluble metals present in uk
477 particulate matter. *Exp. Lung Res.* 31 (7), 671-683.

478 Midander, K., Elihn, K., Wallen, A., Belova, L., Karlsson, A.-K.B., Wallinder, I.O., 2012.
479 Characterisation of nano- and micron-sized airborne and collected subway
480 particles, a multi-analytical approach. *Sci. Total Environ.* 427, 390-400.

481 Minguillon, M.C., Reche, C., Martins, V., Amato, F., de Miguel, E., Capdevila, M.,
482 Centelles, S., Querol, X., Moreno, T., 2018. Aerosol sources in subway
483 environments. *Environ. Res.* 167, 314-328.

484 Mohsen, M., Ahmed, M.B., Zhou, J.L., 2018. Particulate matter concentrations and
485 heavy metal contamination levels in the railway transport system of Sydney,
486 Australia. *Transport. Res. D-Tr. E.* 62, 112-124.

487 MohseniBandpi, A., Eslami, A., Ghaderpoori, M., Shahsavani, A., Jeihooni, A.K.,
488 Ghaderpoury, A., Alinejad, A., 2018. Health risk assessment of heavy metals on
489 PM_{2.5} in Tehran air, Iran. *Data in brief* 17, 347-355.

490 Moreno, T., Kelly, F.J., Dunster, C., Oliete, A., Martins, V., Reche, C., Cruz Minguillon,
491 M., Amato, F., Capdevila, M., de Miguel, E., Querol, X., 2017. Oxidative potential
492 of subway PM_{2.5}. *Atmos. Environ.* 148, 230-238.

493 Moreno, T., Martins, V., Querol, X., Jones, T., BeruBe, K., Cruz Minguillon, M., Amato,
494 F., Capdevila, M., de Miguel, E., Centelles, S., Gibbons, W., 2015. A new look at
495 inhalable metalliferous airborne particles on rail subway platforms. *Sci. Total*
496 *Environ.* 505, 367-375.

497 Moreno, T., Perez, N., Reche, C., Martins, V., de Miguel, E., Capdevila, M., Centelles,
498 S., Minguillon, M.C., Amato, F., Alastuey, A., Querol, X., Gibbons, W., 2014.
499 Subway platform air quality: Assessing the influences of tunnel ventilation, train
500 piston effect and station design. *Atmos. Environ.* 92, 461-468.

501 Namgung, H., Kim, J., Kim, M., Kim, M., Park, S., Woo, S., Bae, G., Park, D., Kwon,
502 S., 2017. Size distribution analysis of airborne wear particles released by subway
503 brake system, *Wear.* 372, 169-176.

504 Olawoyin, R., Schweitzer, L., Zhang, K.Y., Okareh, O., Slaters, K., 2018. Index analysis
505 and human health risk model application for evaluating ambient air-heavy metal
506 contamination in Chemical Valley Sarnia. *Ecotox. Environ. Safe.* 148, 72-81.

507 Palleschi, S., Rossi, B., Armiento, G., Montereali, M.R., Nardi, E., Tagliani, S.M.,
508 Inglessis, M., Gianfagna, A., Silvestroni, L., 2018. Toxicity of the readily leachable
509 fraction of urban PM_{2.5} to human lung epithelial cells: Role of soluble metals.
510 *Chemosphere* 196, 35-44.

511 Pan, S., Du, S.S., Wang, X.R., Zhang, X.X., Xia, L., Liu, J.P., Pei, F., Wei, Y.X., 2019.
512 Analysis and interpretation of the particulate matter (PM₁₀ and PM_{2.5})
513 concentrations at the subway stations in Beijing, China. *Sustain. Cities Soc.* 45,
514 366-377.

515 Reche, C., Moreno, T., Martins, V., Minguillon, M.C., Jones, T., de Miguel, E.,
516 Capdevila, M., Centelles, S., Querol, X., 2017. Factors controlling particle number

517 concentration and size at metro stations. *Atmos. Environ.* 156, 169-181.

518 Saeedi, R., Khani Jazani, R., Khaloo, S.S., Amirkhani Ardeh, S., Fouladi-Fard, R.,
519 Nikukalam, H., 2021. Risk assessment of occupational and public exposures to
520 airborne particulate matter arising from a subway construction site in Tehran, Iran.
521 *Air Qual. Atmos. Hlth.* 14 (6), 855-862.

522 Salma, I., Weidinger, T., Maenhaut, W., 2007. Time-resolved mass concentration,
523 composition and sources of aerosol particles in a metropolitan underground railway
524 station. *Atmos. Environ.* 41 (37), 8391-8405.

525 Shao, L.Y., Hou, C., Geng, C.M., Liu, J.X., Hu, Y., Wang, J., Jones, T., Zhao, C.M.,
526 BeruBe, K., 2016. The oxidative potential of PM₁₀ from coal, briquettes and wood
527 charcoal burnt in an experimental domestic stove. *Atmos. Environ.* 127, 372-381.

528 Shao, L.Y., Li, J., Zhang, M.Y., Wang, X.M., Li, Y.W., Jones, T., Feng, X.L., Silva,
529 L.F.O., Li, W.J., 2021. Morphology, composition and mixing state of individual
530 airborne particles: effects of the 2017 Action Plan in Beijing, China. *J. Clean. Prod.*
531 329 (20), 129748.

532 Shao, L.Y., Li, Y.W., Jones, T., Santosh, M., Liu, P.J., Zhang, M.Y., Xu, L., Li, W.J., Lu,
533 J., Yang, C.-x., Zhang, D.Z., Feng, X.L., Bérubé, A., 2022a. Airborne microplastics:
534 A review of current perspectives and environmental implications. *J. Clean. Prod.*
535 347, 131048.

536 Shao, L.Y., Liu, P.J., Jones, T., Yang, S.S., Wang, W.H., Zhang, D.Z., Li Y.W., Yang, C.
537 -x., Xing, J.P., Hou, C., Zhang, M.Y., Feng, X.L., Li, W.J., Bérubé, K., 2022b. A
538 review of atmospheric individual particle analyses: methodologies and applications
539 in environmental research. *Gondwana Res.* Accepted.
540 <https://doi.org/10.1016/j.gr.2022.01.007>.

541 Schneidemesser, V.E., Stone, E.A., Quraishi, T.A., Shafer, M.M., Schauer, J.J., 2010.
542 Toxic metals in the atmosphere in Lahore, Pakistan. *Sci. Total Environ.* 408 (7),
543 1640-1648.

544 Van Ryswyk, K., Anastasopoulos, A.T., Evans, G., Sun, L., Sabaliauskas, K., Kula, R.,
545 Wallace, L., Weichenthal, S., 2017. Metro commuter exposures to particulate air
546 pollution and PM_{2.5}-associated elements in three canadian cities: the urban
547 transportation exposure study. *Environ. Sci. Technol.* 51 (10), 5713-5720.

548 Van Drooge, B., Prats, R., Reche, C., Minguillon, M., Querol, X., Grimalt, J., Moreno,
549 T., 2018. Origin of polycyclic aromatic hydrocarbons and other organic pollutants
550 in the air particles of subway stations in Barcelona. *Sci. Total Environ.* 642, 148-
551 154.

552 Wang, W.H., Shao, L.Y., Zhang, D.Z., Li, Y.W., Li, W.J., Liu, P.J., Xing, J.P., 2022.
553 Mineralogical similarities and differences of dust storm particles at Beijing from
554 deserts in the north and northwest. *Sci. Total Environ.* 803, 149980.

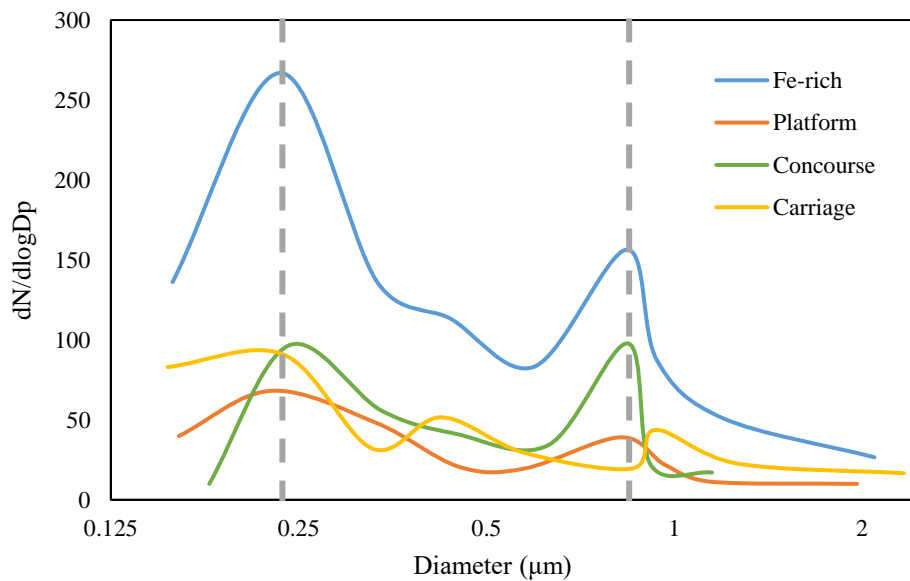
555 Xiao, D., Li, B.X., Cheng, S.X., 2020. The effect of subway development on air
556 pollution: Evidence from China. *J. Clean. Prod.* 275, 124149.

557 Xing, J.P., Shao, L.Y., Zhang, W.B., Peng, J.F., Wang, W.H., Shuai, S.J., Hu, M., Zhang,
558 D.Z., 2020. Morphology and size of the particles emitted from a gasoline-direct-
559 injection-engine vehicle and their ageing in an environmental chamber. *Atmos.*
560 *Chem. Phys.* 20, 2781-2794.

561 Zelikoff, J.T., Schermerhorn, K.R., Fang, K.J., Cohen, M.D., Schlesinger, R.B., 2002.
 562 A role for associated transition metals in the immunotoxicity of inhaled ambient
 563 particulate matter. *Environ. Health Persp.* 110, 871-875.
 564 Zhao, L.J., Wang, J.J., Gao, H. O., Xie, Y.J., Jiang, R., Hu, Q.M., Sun, Y., 2017.
 565 Evaluation of particulate matter concentration in Shanghai's metro system and
 566 strategy for improvement. *Transport. Res. D-Tr. E.*, 53, 115-127.
 567 Zhu, Y.h., Li, W.j., Lin, Q.h., Yuan, Q., Liu, L., Zhang, J., Zhang, Y.X., Shao, L.Y., Niu,
 568 H.Y., Yang, S.S., Shi, Z.B., 2020. Iron solubility in fine particles associated with
 569 secondary acidic aerosols in east China. *Environ. Pollut.* 264, 114769

570
 571
 572
 573
 574
 575
 576
 577
 578
 579
 580
 581
 582
 583
 584
 585

586 Fig. S1. Size distribution of Fe-rich particles in different areas of subway station air
 587 from the TEM analysis.



588